THE EFFECT OF INLET DISTORTION ON 3D ANNULAR DIFFUSERS

Angelina M. Padilla
Department of Mechanical Engineering
Stanford University
488 Escondido Mall, Bldg 500, Stanford, California 94305 USA
angpad@stanford.edu

Christopher J. Elkins
Department of Mechanical Engineering
Stanford University
488 Escondido Mall, Bldg 500, Stanford, California, 94305 USA
celkins@stanford.edu

John K. Eaton
Department of Mechanical Engineering
Stanford University
488 Escondido Mall, Bldg 500, Stanford, California 94305 USA
eatonj@stanford.edu

ABSTRACT

The effect of upstream flow distortion on the performance of practical annular diffusers was examined in order to gain insight on how to design a more robust diffuser. Experiments were conducted in one-fifth sectors of an annular diffuser with a single NACA 0015 airfoil shaped support strut in the center. Three diffusers with different expansion ratios ranging from conservative to aggressive and four inlet conditions were investigated. Magnetic resonance velocimetry was used to measure all three components of time averaged velocity over the entire flow field. The conservative diffuser design was robust in that it did not stall for any of the various inlet conditions. However, there were substantial variations in the flow development. The moderate diffuser stalled for one of the inlet conditions, and the aggressive diffuser stalled for all inlet conditions investigated. The development of the boundary layer along the diffusing wall and the separated wake of the support strut were both very sensitive to varying inlet conditions.

INTRODUCTION

Diffusers are fundamental components of many systems since they are a simple device to recover pressure and decrease velocity. Previous studies have examined many different aspects of diffusers. A detailed study performed by Sovran and Klomp (1967) characterized pressure recovery and generated performance charts for simple 2D rectangular, conical and annular diffusers. Wolf and Johnston (1969) investigated the effect of nonuniform inlet profiles in a 2D rectangular diffuser and found a wide range of performance including both stalled and unstalled flows. Stevens and Williams (1980) investigated the effect of inlet mean velocity profile (from uniform to fully developed) and turbulence on diffuser performance in an annular diffuser and found an increase in pressure recovery with increased levels of turbulence. Cherry et al. (2010) measured the full 3D velocity field in annular diffusers with strut wakes at the diffuser inlet and found little difference in mean velocity for unstalled diffusers. However, all these studies and many more were conducted in diffusers with simple geometries.

In actual applications diffusers have complex 3D geometries, and they may have highly disturbed inlet flows. Sieker and Seume (2008) investigated the effect of swirl angle and rotating blade wakes upstream of a turbine exhaust diffuser which had an annular inlet and a conical outlet. It was found that increasing the swirl number could increase the pressure recovery until flow separation decreased the benefits. Computational models have difficulty predicting flow in adverse pressure gradients, and 3D effects further complicate the problem. A study by Cherry et al. (2008) measured velocity and pressure in a 3D rectilinear diffuser and found the flow was highly sensitive to the upstream secondary flows. Computational models examined as part of the ERCOFTAC workshop in refined turbulence models (Jakirlic´ 2010) were unable to accurately predict the flow except for high order simulations that captured the inlet secondary flows found in the experiment. This suggests that diffuser designs with separation are very sensitive to inlet perturbations. The robustness of a diffuser is directly related to whether or not the

diffuser is separated and how sensitive the separation bubble is to perturbations in the upstream flow. Diffusers designed for optimum pressure recovery generally operate near separation or with some separation present. Therefore it is critical to understand the sensitivity of practical diffuser geometries to a range of inlet disturbances. In order to gain insight into this problem, we measured full three-component mean velocity data throughout the entire flow field in practical annular diffusers to analyze the effect of upstream flow distortion with the objective of learning how to design an efficient yet robust diffuser.

EXPERIMENTAL APPARATUS AND TECHNIQUES

The experiments used magnetic resonance velocimetry (MRV) to measure the three component mean velocity field in diffuser models fabricated using stereolithography (SLA). Because of the efficiency of MRV and the rapid manufacturing capability of SLA, the flow in multiple diffusers with a range of different inlet conditions could be examined. Each test model was a one-fifth sector (or 72^o arc) of an annular diffuser and contained a single, truncated NACA 0015 shaped support strut that passed through the center of the sector. The strut was representative of struts that support the centerbody in practical applications. The diffusers had an inlet OD/ID of 2.0 and a non-dimensional length of L/H=1, where H=30 mm was the annulus height at the diffuser inlet. The diffusers had a straight inner wall and a single expanding wall at the outer radius. Each diffuser had a high initial expansion angle of the outer wall to maximize pressure recovery approaching the strut and then halfway through the diffuser the angle was decreased to 6^o to prevent separation. The conservative diffuser had an initial expansion angle of 12^o, the moderate diffuser 16^o and the aggressive diffuser 20^o. These expansion angles yielded exit area ratios of 1.21, 1.29 and 1.34, respectively. A photograph and a schematic of the diffusers are in Figure 1.

The recirculating flow system in Figure 2 was designed to supply a steady, uniform flow with thin boundary layers and low turbulence intensity at the diffuser inlet. The inlet assembly provided nearly uniform flow to a 76 mm diameter by 0.3 m long straight tube that fed a 2.7:1 area ratio contraction. The contraction morphed the cross-sectional area from a circle into an annular sector. An optional inlet perturbation device could be placed upstream of the test diffuser. The diffuser dumped into an exit plenum with a rectangular cross section.

Three different inlet perturbation devices were designed to roughly mimic conditions found in turbine exhaust diffusers. The first perturbation device was a nonuniform grid followed by a constant cross-section duct 5.9H long. The nonuniform grid had low blockage at small radii and high blockage at large radii generating a velocity gradient with decreasing velocity with increasing radius. The difference between the maximum and minimum velocity outside of the boundary layers was about 17% and the turbulence intensity was 4.4%. The second perturbation device generated a thin wall jet at the

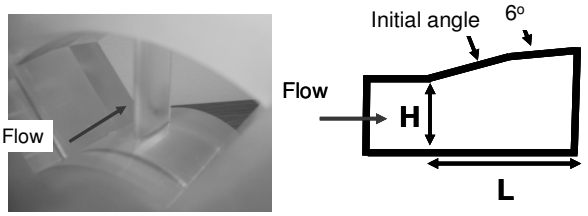

Figure 1: Photograph of diffuser (left) and schematic of diffuser (right).

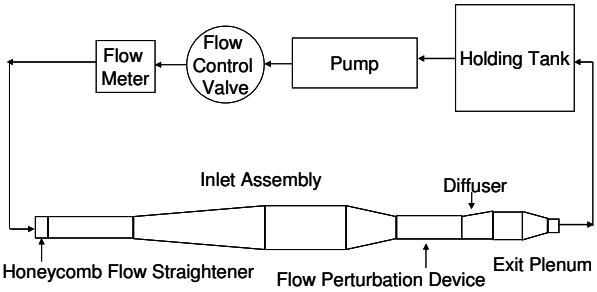

Figure 2: Schematic of flow setup

outer radius of the sector representing flow escaping around the tip of the turbine blades in the actual application. The device was supplied from a second pump and flowmeter and produced a jet 0.03H thick with a maximum velocity 1.4 times the bulk velocity. The jet exit was located 0.9H upstream of the diffuser inlet. The third device was a turbulence generation grid with vortex generators. The grid was located in a constant cross-sectional duct 3.5H long. The grid increased the turbulence intensity to about 7% while maintaining nominally uniform mean flow. Freestream turbulence levels for the uniform and tip jet flows were approximately 3%.

The entire flow system was made of plastic to avoid interference with the MRI scanner used to make the velocity measurements. The diffuser models and most other parts were fabricated using stereolithography (SLA) at the Keck Laboratory at the University of Texas, El Paso.

The working fluid was a 0.06 molar solution of copper sulfate in water and it was maintained at 25 ^{o}C throughout the experiment. Copper sulfate is an MRI contrast agent that increases the signal to noise ratio. The Reynolds number based on the bulk inlet velocity of 1.66 m/s and the diffuser height (H = 30 mm) at the inlet was 49,000.

The velocity measurements were acquired using phase-contrast MRV (Elkins et al., 2003) at the Richard M. Lucas Center for Imaging at Stanford University. A 1.5-T MR system (GE Signa CV/i, Gmax = 40 mT/m, rise time = 268 μs) along with a transmit receive head coil were used to measure the three component velocity field on a regular Cartesian mesh. The data were collected in a field-of-view that was 23.9 cm in the streamwise direction by 8.9 cm in the vertical direction by 12.0 cm in the horizontal direction. This volume was divided into a uniform grid with a spacing of 0.9

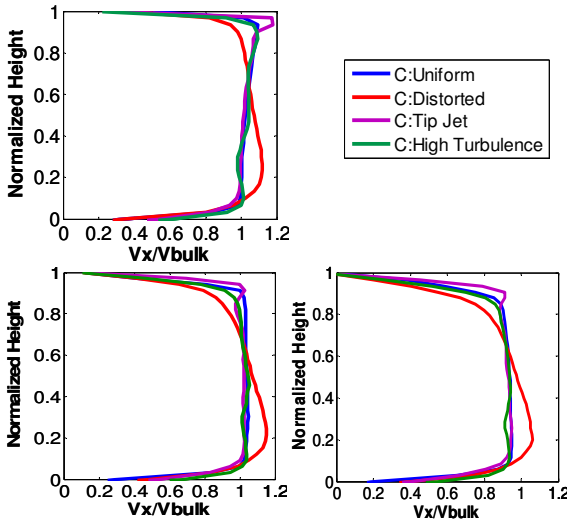

Figure 3: Circumferentially averaged streamwise velocity profiles at diffuser inlet (top), halfway through diffuser (bottom left) and diffuser outlet (bottom right).

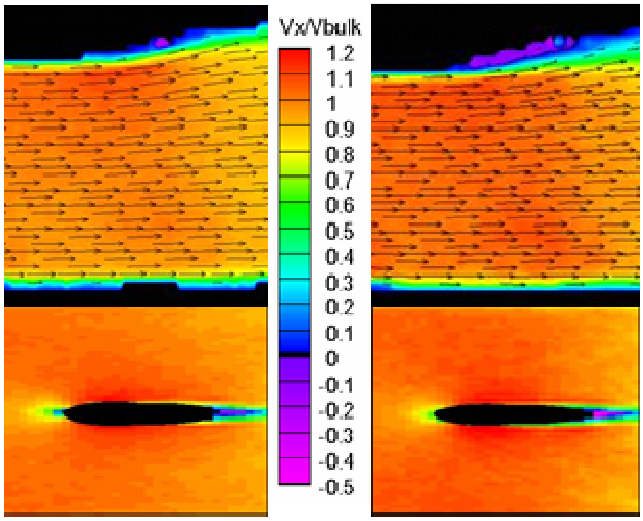

Figure 4: Contours of axial velocity for the uniform inlet case along the length of the diffuser. Contours and in-plane vectors in a plane at a constant angle halfway between the strut and the sector wall for the conservative (top left) and moderate (top right) diffusers. Velocity contours at H/2 for the conservative diffuser (bottom left) and the moderate diffuser (bottom right).

mm in each direction. The diffuser assembly was placed in the magnet so the measuring volume spanned from upstream of the diffuser inlet to just downstream of the diffuser outlet. Fiducial marks fabricated into the diffuser walls were used to orient the flow data relative to the diffuser geometry within 0.5 mm.

Four complete sets of three-component mean velocity data were measured for each diffuser. Each of the four scans took approximately 12 minutes. Before each data set and after the final data set an additional MRI scan was measured with the fluid stationary. Consequently, there were four "flow-on" measurements and five "flow-off" measurements. The flow-off data acquired before and after each flow-on case were averaged together and then subtracted from the bracketed flow-on data to correct for any biasing due to eddy currents induced by the MRI pulse sequence. Then the corrected data sets were averaged together to yield a single final data set. A velocity uncertainty of 5.8% for a typical final data set was estimated using a 95% confidence interval and a standard deviation calculated using the method described in Elkins et al. (2007). These estimates were corroborated by comparing the flowrate measured using the supply flowmeter to that calculated by integrating the velocity field across planes. Agreement at all streamwise positions was within 3%.

The turbulence measurements were taken in a separate air flow experiment that used the same test section and operated at the same Reynolds number as the MRV experiments. An A.A. Lab Systems hot-wire bridge was used with a standard Dantec 55P single wire probe which had a 2 mm long by 5 micron diameter wire. The anemometer was calibrated against a pitot static probe in a uniform jet flow which was connected to a manometer with a max range of 30 and a resolution of 0.1 inches of water. Five thousand velocity samples were taken at a rate of 180 samples a second for each measurement location.

RESULTS

The velocity measurements for the conservative diffuser with the four inlet conditions are summarized in Figure 3 as radial plots of the circumferentially-averaged streamwise velocity. The vertical axis is the normalized local annulus height and the horizontal axis is the streamwise velocity normalized by the inlet bulk velocity. The top plot in Figure 3 is at the inlet to the diffuser. All four cases had relatively thin boundary layers at the inlet. The baseline, jet and higher turbulence cases had nearly identical velocity profiles except within the jet at the outer radius. The distorted case had a core velocity which decreased slowly with radius. The subsequent plots in Figure 3 show the development of the velocity profile through the diffuser. These plots show that the diffuser amplified distortions in the core flow. This is evident for the distorted mean profile case where the velocity gradient in the core increased. The wall jet diffused while moving downstream, but it was still evident at the diffuser exit. The largest difference between the four cases was that the boundary layer grew more rapidly for the distorted case and less rapidly for the jet case. The boundary layer growth for the uniform and higher turbulence cases was nearly the same. This suggests that the distorted case would be the most likely to separate. However, the conservative diffuser did not stall under any of the inlet conditions investigated.

The moderate diffuser did separate with the uniform inlet. This is illustrated in Figure 4 which compares axial velocity contours along the length of the conservative and moderate

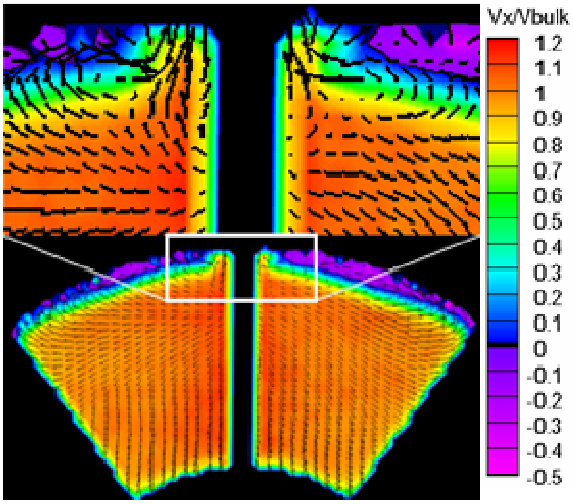

Figure 5: Axial velocity contours and adjusted in-plane vectors at x/L=0.55 in moderate diffuser with uniform inlet. Entire cross-section (bottom), zoomed-in view (top).

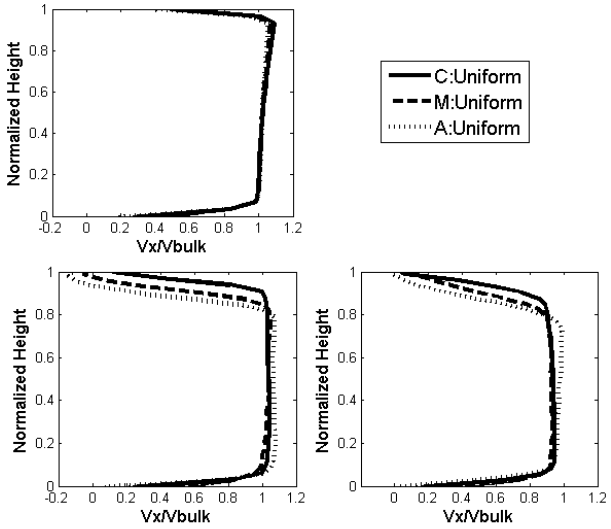

Figure 6: Circumferentially averaged streamwise velocity profiles for uniform velocity inlet for all three diffusers at diffuser inlet (top), halfway through diffuser (bottom left) and diffuser outlet (bottom right).

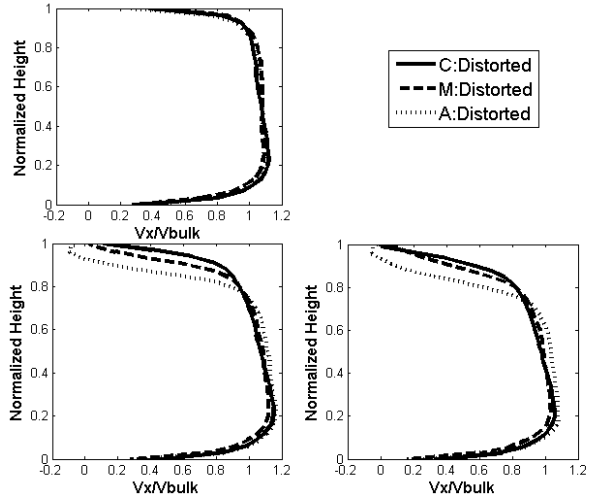

Figure 7: Circumferentially averaged streamwise velocity profiles for distorted velocity inlet for all three diffusers at diffuser inlet (top), halfway through diffuser (bottom left) and diffuser outlet (bottom right).

diffusers for a uniform inlet. In the conservative case the flow accelerated slightly as it flowed around the upstream half of the strut, due to the overall decrease in area even though the outer wall was expanding. There was a small amount of reverse flow but it was not stalled. The moderate diffuser was stalled in the 16° expansion region, but not in the 6° expansion region. The vectors indicate the flow only turned slightly towards the expanding wall in both cases and there was less turning in the moderate diffuser than there was in the conservative diffuser.

The bottom two plots in Figure 4 are streamwise velocity contours at a constant radius of H/2. Both cases were very similar. The contours were nearly identical at this location despite the fact that one of the diffusers was stalled and the other was not. The primary difference between the contours was the magnitude. The moderate diffuser had slightly faster positive and negative velocities. There were slightly faster velocities around the middle of the strut for the moderate case compared to the conservative case. There were also faster reverse flow velocities in the wake of the strut which resulted in slower forward flow in the wake of the strut at the outlet of the diffuser.

A plane near the end of the separation bubble, x/L=0.55, for the moderate diffuser with uniform inlet is shown in Figure 5. The bottom plot shows that the reverse flow region spanned the entire top of the diffuser except where the strut intercepted the top wall. The adjusted in-plane velocity vectors overlaid in Figure 5 were calculated by subtracting the vertical component due to the expanding wall as $V_{y,a}=V_y-V_x\sin(\theta_{wall})$. The horizontal velocity component remained unchanged. For the plane of data in Figure 5, θ_{wall} was 6°. The top plot in Figure 5 shows a zoomed-in region around the strut at the top of the annulus. The adjusted in plane vectors show evidence of two counter rotating vortices that swept up higher velocity fluid from the core region towards the strut and the expanding walls and kept the separation bubble away from the strut wall.

The velocity profile development through each of the three diffusers with the uniform inlet is shown in Figure 6. The plots show that the inlet was the same for all three diffusers, but significant differences had developed by halfway through the diffuser. The conservative diffuser had the thinnest boundary layer and no reverse flow. The moderate and aggressive diffusers had slow reverse flow

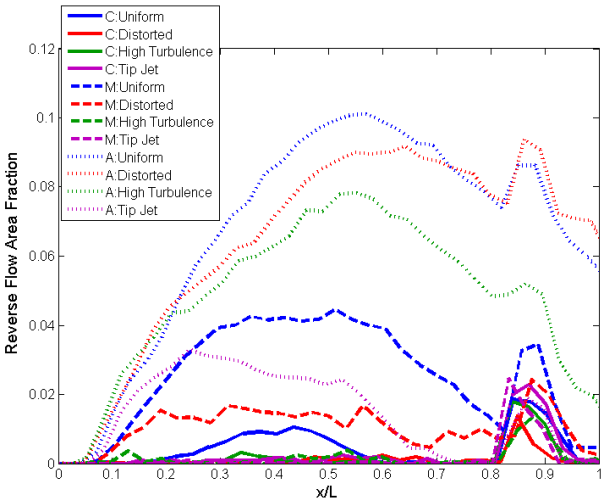

Figure 8: Fractional area of reverse flow for all twelve cases.

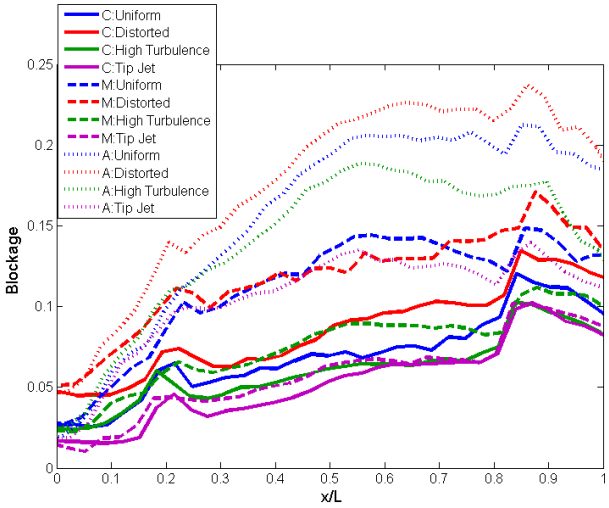

Figure 9: Blockage for all twelve cases.

regions with the aggressive diffuser having greater reverse flow than the moderate diffuser. At the outlet of the diffuser, the aggressive diffuser still had reverse flow and a thick boundary layer. The conservative and moderate diffusers did not have any reverse flow, but the moderate diffuser had a thicker boundary layer.

A similar set of plots of the velocity profile development through all three diffusers for the distorted inlet condition is shown in Figure 7. The top plot once again shows the variation in the inlet condition for each of the diffusers. The bottom left plot shows the velocity profile development halfway through the diffuser. Unlike the uniform inlet condition only the aggressive diffuser had reverse flow. The moderate diffuser was not separated for this inlet condition although it did have a slightly thicker boundary layer than the conservative diffuser. At the outlet of the diffuser there was little difference between the velocity profile for the conservative and moderate diffusers for a normalized annulus height. Similar to the uniform inlet case the aggressive diffuser still had reverse flow at the outlet of the diffuser, and it had a much thicker boundary layer than the other two diffusers.

Figure 8 shows the fraction of the cross section occupied by reverse flow for the twelve cases. The end of the strut was at x/L=0.85 which is why there was a sharp increase in reverse flow area of about 2% for each case at that location. The expansion angle at the outer wall decreased halfway through the diffuser which caused the reduction in reverse flow for each case in the second half of the diffuser. The inlet condition that yielded the highest fraction of reverse flow was the uniform inlet. The conservative diffuser was not stalled and, with the exception of the strut wake region, only had a small amount of reverse flow of less than 0.01 for the uniform inlet case. The moderate diffuser was stalled for the front half of the diffuser and had a maximum reverse flow fractional area of 0.045 halfway through the diffuser. The aggressive diffuser was stalled along the entire length of the diffuser and had a maximum reverse flow area fraction of 0.1. In each diffuser, the distorted velocity profile at the inlet reduced the amount of reverse flow. This was contrary to what was expected. However, for this inlet condition elevated turbulence levels caused by the grid used to generate the mean profile most likely contributed to the reduction in reverse flow. This is most notable for the moderate diffuser which had over a 60% reduction in reverse flow and was no longer stalled. The high turbulence and tip jet cases eliminated the reverse flow for the moderate diffuser and decreased the size of the separation bubble for the aggressive diffuser. The tip jet case resulted in the smallest separation bubble for the aggressive diffuser.

The blockage was calculated using a method adapted from Khalid et al. (1999) The method calculates the velocity gradient field in order to determine the "freestream" or core velocity. The core region at each streamwise position was defined as the region with the lowest gradient magnitudes excluding any areas of reverse flow. Instead of using the velocity at the edge of the core region as described in Khalid et al. (1999), the mean streamwise velocity within the core region, Uc, was calculated and used in Equation 1 to calculate the blocked area. The blockage in Figure 9 is the blocked area divided by the cross-sectional area at each streamwise position.

$$A_b(x) = \int\int (1 - \frac{V_x}{U_c}) dA \qquad (1)$$

The blockage plotted in Figure 9 shows that the minimum blockage occurred for the conservative diffuser, specifically the case with the tip jet. For this case the blockage at the inlet to the diffuser was 0.017 compared to 0.027 for the

conservative case with the uniform inlet. The highest blockage value in the diffuser occurred just after the end of the strut and the distorted inlet condition yielded the highest values of the four inlet conditions. The maximum blockage for each diffuser was 0.13 for the conservative diffuser, 0.17 for the moderate diffuser and 0.24 for the aggressive diffuser.

CONCLUSION

The effect of inlet distortion was investigated in three annular diffuser sectors with a single strut. It was found that for the uniform inlet condition there was some reverse flow in all three diffusers; however, only the moderate and aggressive diffusers were actually stalled. The presence of the strut resulted in a small reverse flow region in the wake of the strut and counter rotating vortices along the sides. The separation bubble in the wake varied in length depending on the inlet condition but did not reach the outlet. The vortices prevented the separation bubble, in cases which had one, to reach all the way to the strut wall.

When there was a distorted velocity profile, tip jet or increased turbulence at the inlet, only the aggressive diffuser stalled. For the distorted velocity profile, this was due in part to the somewhat higher levels of turbulence for this inlet condition compared to the uniform inlet. The blockage tended to be highest for this inlet condition except for the moderate diffuser where it was comparable to the uniform inlet case because it was stalled. The tip jet case had the thinnest boundary layer along the diffusing wall and the least amount of blockage overall.

Both the conservative and aggressive diffusers were robust while the moderate diffuser was not. The conservative diffuser never stalled regardless of the inlet condition and similarly the aggressive diffuser always stalled. The flow behavior for the moderate diffuser, however, varied greatly depending on the inlet condition. For the uniform inlet case the diffuser was stalled, for the distorted velocity case there was some reverse flow but it was no longer stalled, and for the high turbulence and tip jet cases the only reverse flow was in the wake of the strut. The blockage also varied greatly. Overall, this diffuser's performance in a practical application would be very difficult to predict.

ACKNOWLEDGEMENTS

We would like to thank Siemens Energy Inc., the Bill and Melinda Gates Foundation and the Alfred P. Sloan Foundation for their financial support.

REFERENCES

Cherry, E. M., Elkins, C. J., and Eaton, J. K., 2008, "Geometric Sensitivity of Three-Dimensional Separated Flows", *International Journal of Heat and Fluid Flow*, Vol. 29, pp. 803-811.

Cherry, E. M., Padilla, A. M., Elkins, C. J., and Eaton, J. K., 2010, "Three-Dimensional Velocity Measurements in Annular Segments Including the Effects of Upstream Strut Wakes", *International Journal of Heat and Fluid Flow*, Vol. 31, pp. 569-575.

Elkins, C. J., Markl, M., Pelc, N., and Eaton, J. K., 2003, "4D Magnetic Resonance Velocimetry for Mean Velocity Measurements in Complex Turbulent Flows," *Experiments in Fluids*, Vol. 34, pp. 494-503.

Elkins, C. J., Alley, M. T., 2007, "Magnetic Resonance Velocimetry: Applications of Magnetic Resonance Imaging in the Measurement of Fluid Motion", *Experiments in Fluids*, Vol. 43, pp. 823-858.

Jakirlic´, S., Kadavelil, G., Sirbubalo, E., von Terzi, D., Breuer, M., and Borello., D., 2010, "14th ERCOFTAC SIG15 Workshop on Turbulence Modelling: Turbulent Flow Separation in a 3-D diffuser", *ERCOFTAC Bulletin*, Vol. 82.

Khalid, S. A., Khalsa, A. S., Waitz, I. A., Tan, C. S., Greitzer, E. M., Cumpsty, N. A., Adamczyk, J. J., and Marble, F. E., 1999, "Endwall Blockage in Axial Compressors", *ASME Journal of Turbomachinery*, Vol. 121, pp. 499-509.

Sieker, O. and Seume, J. R., 2008, "Effects of Rotating Blade Wakes on Separation and Pressure Recovery in Turbine Exhaust Diffusers", *Proceedings of ASME Turbo Expo 2008: Power for Land, Sea and Air*, GT2008-50788.

Sovran, G. and Klomp, E. D., 1967, "Experimentally Determined Optimum Geometries for Rectilinear Diffusers with Rectangular, Conical or Annular Cross-Section", *Fluid Mechanics of Internal Flows*, Elsevier Publishing, New York, pp. 270-319.

Stevens, S. J., and Williams, G. J., 1980, "The Influence of Inlet Conditions on the Performance of Annular Diffusers", *ASME Journal of Fluids Engineering*, Vol. 102, pp. 357-363.

Wolf, S., and Johnston, J. P., 1969, "Effects of Nonuniform Inlet Velocity Profiles on Flow Regimes and Performance in Two-Dimensional Diffusers", *Transactions of the ASME, Journal of Basic Engineering*, Vol. 91, pp. 462-474.